frontiers | Frontiers in Astronomy and Space Sciences

TYPE Mini Review
PUBLISHED 31 July 2024
DOI 10.3389/fspas.2024.1436916



OPEN ACCESS

EDITED BY
Alla V. Suvorova,
National Central University, Taiwan

REVIEWED BY
Zhaojin Rong,
Institute of Geology and Geophysics,
Chinese Academy of Sciences (CAS), China

*CORRESPONDENCE
Primož Kajdič,
primoz@igeofisica.unam.mx

RECEIVED 22 May 2024
ACCEPTED 12 July 2024
PUBLISHED 31 July 2024

CITATION
Kajdič P, Blanco-Cano X, Turc L, Archer M, Raptis S, Liu TZ, Pfau-Kempf Y, LaMoury AT, Hao Y, Escoubet PC, Omidi N, Sibeck DG, Wang B, Zhang H and Lin Y (2024), Transient upstream mesoscale structures: drivers of solar-quiet space weather.
*Front. Astron. Space Sci.* 11:1436916.
doi: 10.3389/fspas.2024.1436916



# Transient upstream mesoscale structures: drivers of solar-quiet space weather

Primož Kajdič[1]*, Xóchitl Blanco-Cano[1], Lucile Turc[2], Martin Archer[3], Savvas Raptis[4], Terry Z. Liu[5], Yann Pfau-Kempf[2], Adrian T. LaMoury[3], Yufei Hao[6], Philippe C. Escoubet[7], Nojan Omidi[8], David G. Sibeck[9], Boyi Wang[10], Hui Zhang[11] and Yu Lin[12]

[1]Departamento de Ciencias Espaciales, Instituto de Geofísica, Universidad Nacional Autónoma de México, Mexico City, Mexico, [2]Department of Physics, University of Helsinki, Helsinki, Finland, [3]Blackett Laboratory, Imperial College London, London, United Kingdom, [4]The Johns Hopkins University Applied Physics Laboratory, Laurel, MD, United States, [5]Department of Earth, Planetary, and Space Science, University of California, Los Angeles, Los Angeles, CA, United States, [6]Purple Mountain Observatory, Chinese Academy of Sciences (CAS), Nanjing, China, [7]ESA/ESTEC, Noordwijk, Netherlands, [8]Solana Scientific Inc., Solana Beach, CA, United States, [9]NASA Goddard Space Flight Center, Greenbelt, MD, United States, [10]Institute of Space Science and Applied Technology, Harbin Institute of Technology (Shenzhen), Shenzhen, China, [11]School of Space Science and Physics, Shandong University, Weihai, China, [12]Physics Department, Auburn University, Auburn, AL, United States

In recent years, it has become increasingly clear that space weather disturbances can be triggered by transient upstream mesoscale structures (TUMS), independently of the occurrence of large-scale solar wind (SW) structures, such as interplanetary coronal mass ejections and stream interaction regions. Different types of magnetospheric pulsations, transient perturbations of the geomagnetic field and auroral structures are often observed during times when SW monitors indicate quiet conditions, and have been found to be associated to TUMS. In this mini-review we describe the space weather phenomena that have been associated with four of the largest-scale and the most energetic TUMS, namely, hot flow anomalies, foreshock bubbles, travelling foreshocks and foreshock compressional boundaries. The space weather phenomena associated with TUMS tend to be more localized and less intense compared to geomagnetic storms. However, the quiet time space weather may occur more often since, especially during solar minima, quiet SW periods prevail over the perturbed times.

KEYWORDS

**bow shock, transient upstream mesoscale structures, solar-quiet space weather, foreshock, solar wind**

## 1 Introduction

For decades, space weather phenomena have been thought to be strictly related to solar activity. This is mainly due to the fact that the strongest magnetospheric and ionospheric disturbances, geomagnetic storms and substorms (e.g., Akasofu, 2021), occur during the passage of large-scale structures (of the order of ≳1 a. u.) in the solar wind (SW), such as interplanetary coronal mass ejections, stream interaction regions and interplanetary shocks (e.g., Kilpua et al., 2017). During such events, most extreme conditions conducive for space weather, such as large southward IMF, high speed solar wind, and large dynamic pressure ($P_{dyn}$) fluctuations, may be met. This in turn drives strong magnetopause motion and reconnection.

Geomagnetic storms and substorms have been a subject of extensive research for a long time because they can interfere with our technologies by disrupting the proper functioning of, for example, electric grids, GPS signals, and artificial satellites (e.g., Eastwood et al., 2017).

However, in recent years it has become clear that some space weather phenomena, such as bursts of large-amplitude magnetospheric ultra-low-frequency (ULF) pulsations, transient (nonperiodic) geomagnetic disturbances, auroras, *etc.*, may occur in the absence of known space weather drivers (Zhang and Zong, 2020). Since their origin is not related to solar disturbances, we here refer to them as solar-quiet space weather.

Such phenomena may be caused by transient upstream mesoscale structures (TUMS). These form in the region upstream of the bow-shock of Earth. The term mesoscale refers to their typical scale sizes ranging form ~2000 km to more than 10 Earth radii (1 $R_E$ ~ 6400 km) (Zhang and Zong, 2020). The sizes of the largest TUMS are thus comparable to but smaller than the transverse diameter of the dayside magnetosphere (~30 $R_E$ Tsyganenko, 2014).

TUMS owe their existence to the collisionless bow-shock that stands in front of our planet. The bow-shock dissipates some of the SW kinetic energy by deflecting and energizing a small portion of the incident particles (electrons, ions). At its Qpar section, where the angle between the upstream IMF and the local shock normal is less than 45°, reflected particles may escape back upstream to large distances where they coexist with the incoming SW. Such non-Maxwellian particle distributions lead to different instabilities, forming a highly perturbed foreshock region (Eastwood et al., 2005).

The formation mechanisms for TUMS fall into three categories: (1) the interaction of IMF directional discontinuities in the SW (Borovsky, 2008) with the bow-shock or (2) with the reflected foreshock ions and (3) due to internal foreshock processes.

The main reason why TUMS have such an impact on the near-Earth environment is the variation in magnetic field orientation and strength and the SW $P_{dyn}$ inside them which lead to modifications of the total (dynamic, thermal and magnetic) pressure impinging upon the magnetopause (e.g., Archer et al., 2014). As has been shown in the past, upstream negative and positive pressure pulses excite toroidal and poloidal mode waves in the Pc5 frequency range (Zong, 2010; Zhang et al., 2010a). Even modest positive pressure pulses may also lead to an increase in temperature anisotropy of energetic protons which in turn results in ion-cyclotron instability and consequently in Pc1 magnetospheric waves (Olson and Lee, 1983; Anderson and Hamilton, 1993).

$P_{dyn}$ variations have also been found to generate field aligned currents (FACs, Araki, 1994; Nishimura et al., 2016) and intensify whistler mode waves (Li et al., 2011; Shi et al., 2014). FACs can lead to electron precipitation and discrete auroras, while the intensified whistler mode waves can scatter electrons into loss cones and induce diffuse auroras.

Finally, it should be mentioned that various types of TUMS have been observed at other planets, (e.g., Øieroset et al., 2001; Masters et al., 2008; Slavin et al., 2009; Collinson et al., 2012; Collinson et al., 2014; Collinson et al., 2015; Collinson et al., 2020; Uritsky et al., 2014; Valek et al., 2017; Shuvalov et al., 2019; Omidi et al., 2020; Madanian et al., 2023), although their impact on the corresponding downstream regions has not been studied due to the lack of multi-spacecraft observations.

It is the purpose of this mini review to summarize the impact of the largest-scale TUMS on the near-Earth environment. In the following sections we describe such effects caused by hot flow anomalies (HFA, section 2), foreshock bubbles (FB, 3), foreshock compressional boundaries (FCB, 4), and travelling foreshocks (TF, 5). The HFAs and TFs fall into the first category in terms of their formation mechanisms, FBs fall into the second category, while the FCBs occur due to internal foreshock processes. In section 6 we summarize these effects while in section 7 we list some of the future tasks needed to be done in order to deepen our knowledge about the subject.

## 2 Hot flow anomalies

HFAs (Schwartz et al., 1985; Thomsen et al., 1986), form when an IMF directional discontinuity intersects the bow shock and the convection electric field ($-\mathbf{V}\times\mathbf{B}$) points towards the discontinuity's current sheet on at least one side. Their typical sizes range between 1 and 3 $R_E$ in the direction perpendicular to their current sheet, but they have been observed by Chu et al. (2017) to extend up to 7 $R_E$ upstream of the bow shock. HFAs are characterized by (see also Figure 1A) central cores that contain hot plasma with flow velocities much lower than the ambient SW. The plasma flow inside HFAs is by definition highly deflected from the Sun-Earth line. The plasma density and magnetic field values in the core are lower than in the SW. The core is surrounded by a rim in which magnetic field strength and plasma density are enhanced compared to ambient SW values. An example of an HFA is shown in Figure 1A.

The first geoeffective HFA was reported by Sibeck et al. (1998), Sibeck et al. (1999), Borodkova et al. (1998), Sitar et al. (1998). An order of magnitude decrease of the $P_{dyn}$ inside the event caused the magnetopause to move outward and then inward in excess of 5 $R_E$ past Interball-1 twice within 7 min. Minor disturbances in geomagnetic field magnitude were observed at geosynchronous orbit by GOES-8, while Polar Ultraviolet Imager (UVI) observed a sudden brightening of the afternoon aurora, followed by a more intense transient brightening of the morning aurora.

Jacobsen et al. (2009) reported observations of extreme motion of the dawn flank magnetopause caused by an HFA. The magnetopause moved outward by at least 4.8 $R_E$ in 59 s, implying flow speeds of up to 800 km $s^{-1}$ in the direction normal to the nominal magnetopause. The transient deformation of the magnetopause generated field-aligned currents (FACs) and created travelling convection vortices (e.g., Glassmeier et al., 2001) which were detected by ground magnetometers.

Magnetopause deformation due to HFAs was also observed by Šafránková et al. (2012). The authors reported a highly asymmetric deformation of the magnetosphere and suggested that it occurred either due to one elongated HFA or a pair of HFAs

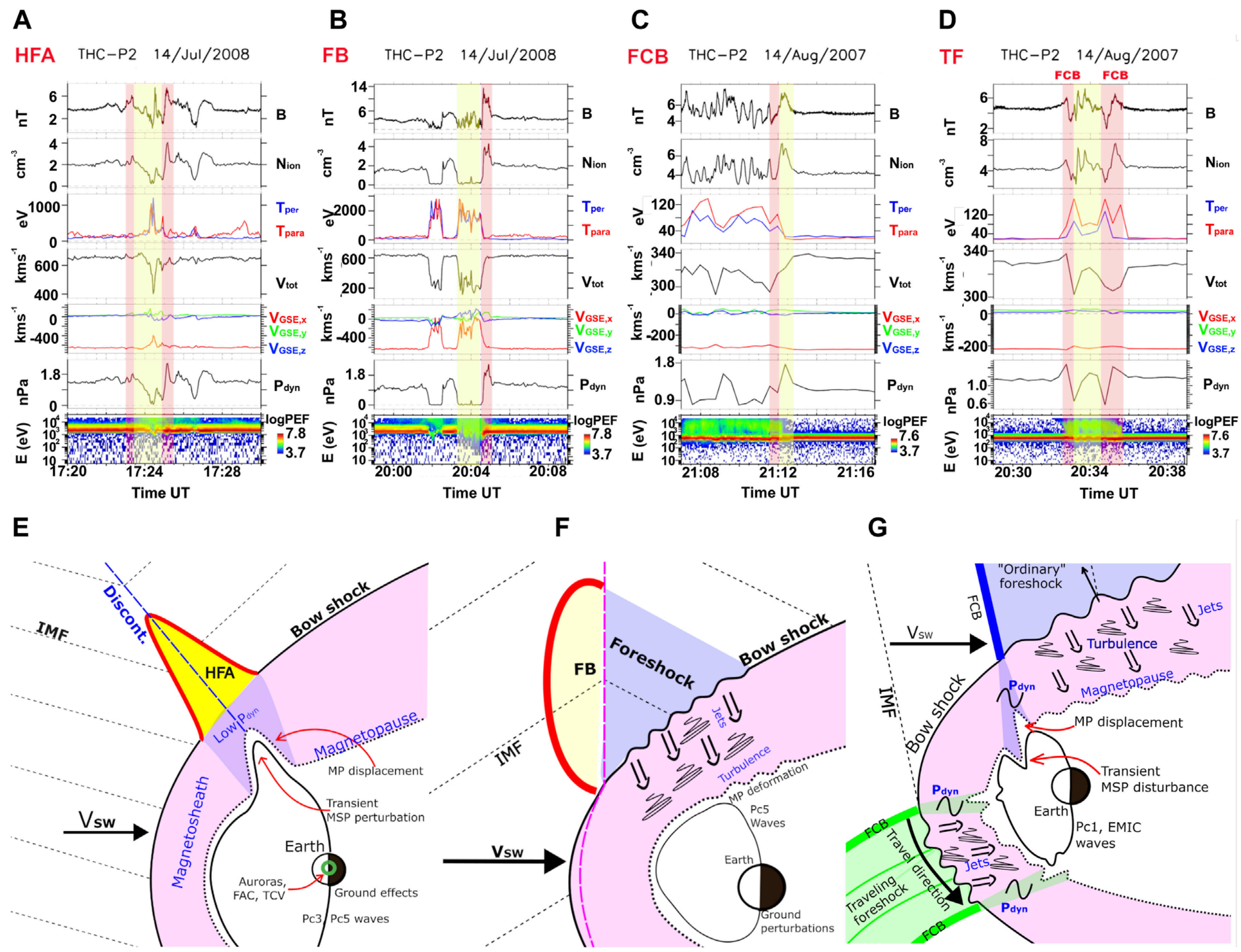


FIGURE 1
(A) Examples of observed (A) HFA, (B) FB, (C) FCB and (D) TF. Sketches of (E) HFA, (F) FB and (G) TF and FCB and the corresponding downstream effects. The panels (A–D) exhibit (form top to bottom) magnetic field magnitude, plasma density, parallel (blue) and perpendicular (red) ion temperatures, SW speed, SW velocity components, SW $P_{dyn}$ and ions spectra. In the case of the HFA and FB, the red shaded intervals mark rims of enhanced B and plasma density, while yellow shaded intervals mark hot cores. In the case of the FCB, the intervals shaded in red and yellow mark the B and density dip and peak, respectively. In the case of the traveling foreshock, the yellow color marks its core, while the red color marks the surrounding FCBs.

that simultaneously appeared at both flanks. On the dusk side, the deformation was very weak. On the dawn side, the magnetopause was first displaced outward from its nominal position by ~5 $R_E$ and then inward by ~4 $R_E$.

Hartinger et al. (2013) and Shen et al. (2018) observed HFAs that excited global Pc5 perturbations (periods 150–600 s, e.g., Jacobs et al., 1964) at the geosynchronous orbit. Hartinger et al. (2013) also reported observations of magnetopause surface modes caused by an HFA. Shen et al. (2018) demonstrated that HFAs can also generate localized magnetospheric oscillations in the Pc5 range with clear dawn-dusk asymmetry.

Several works also related passing HFAs to geomagnetic pulsations in the Pc3 range (22–100 mHz). Eastwood et al. (2011) reported observations of an HFA associated with a type of Pc3 fluctuations whose frequency did not depend on the IMF strength, contrary to the case of Pc3 waves typically observed inside the magnetosphere (e.g., Takahashi et al., 1984). Similarly, Zhao et al. (2017) reported observations of an HFA causing nearly monochromatic Pc3 ULF waves that were observed in orbit and on the ground and that exhibited characteristics of standing Alfvén waves. They occurred in all sectors (dawn, noon, dusk and nightside) indicating that the HFA cause a global response of the magnetosphere.

HFAs have also been shown to impact the nightside magnetosphere. This was first reported by Facskó et al. (2015) who observed an HFA remnant in the far magnetotail at $X \sim -310\ R_E$. Similarly, impacts of unidentified TUMS, possibly HFAs, in the midtail magnetosheath have also been reported by Wang et al. (2018) and Liu et al. (2020, 2021), implying that HFAs may exhibit lifetimes of several tens of minutes.

Figure 1E) summarizes the reported downstream effects of HFAs.

## 3 Foreshock bubbles

Foreshock bubbles (FBs) form due to the interaction of IMF directional discontinuities with the backstreaming foreshock ions.

When the they cross a discontinuity and project their velocity in the new perpendicular direction more than in the new parallel direction, the foreshock ions become more concentrated and thermalized on the upstream side of the discontinuity. Foreshock ions can easily cross rotational discontinuities (RD), since there exists a normal magnetic field component, so the ions can simply propagate along the field lines through them. At tangential discontinuities (TD), the normal magnetic field component is zero, so only ions with gyroradii larger than the TD thickness are able to cross the TDs. (Omidi et al., 2010; Liu et al., 2015; Liu et al., 2016; Wang et al., 2020; Wang et al., 2021). Thus, stronger energy fluxes of foreshock ions are expected across RDs which may cause faster expansion of RD-driven FBs compared to TD-driven FBs.

Once ions cross the discontinuities, they undergo additional heating and start to expand against the SW, forming the bubble. FBs exhibit signatures in spacecraft data that are similar to those of HFAs (see Figure 1B), namely, a hot, tenuous core with low IMF strength and a rim with enhanced density and B-magnitude (see Figure 1B). However, whereas HFAs commonly exhibit rims on their upstream and downstream edges, the FBs only exhibit them on their upstream side. FBs may affect the magnetopause on larger scales than HFAs since their sizes transverse to the Earth-Sun line are larger (5–10 $R_E$ Archer et al., 2015; Turner et al., 2020).

The first to report that FBs can be geoeffective were Hartinger et al. (2013). The authors showed that a FB caused magnetopause undulations. Inside the magnetosphere but close to the magnetopause, the event caused variations of the North-South component of the magnetic field and similar effects were observed at geosynchronous orbit. Pc5 pulsations with similar properties as those commonly associated by the HFAs, were also observed.

Archer et al. (2015) showed that FBs have a global impact on Earth's magnetosphere. Once an FB interacts with the bow shock, magnetosheath particles are accelerated towards the intersection of the FB's current sheet with the bow shock resulting in fast, sunward flows as well as outward motion of the magnetopause. Ground-based magnetometers can detect signatures of this motion simultaneously across 7 h of magnetic local time.

Figure 1F) summarizes the reported downstream effects of FBs.

## 4 Foreshock compressional boundaries

The FCBs (e.g., Omidi et al., 2009, see also Figure 1C) are boundary regions that separate the highly disturbed ultra-low frequency (ULF, Greenstadt et al., 1995) wave foreshock from either the pristine SW or the foreshock region populated by field-aligned ion beams (Paschmann et al., 1980) but not the ULF waves. FCBs are characterized by a strong compression of magnetic field magnitude and density that is followed by strong decreases of these two quantities on the foreshock side (Figure 1C). These events differ somewhat from the rest of the TUMS in the sense that they are not truly transient phenomena. Models indicate that they exist even during steady solar wind conditions and it is their motion, due to changing solar wind conditions, that has a transient impact on the magnetosphere.

Hartinger et al. (2013) described two FCBs that were observed to have an impact on the magnetopause and inside the magnetosphere. Both caused the Themis-D probe, originally located near the magnetopause on the magnetospheric side, to briefly enter the magnetosheath. Transient magnetic field and plasma density perturbations were detected throughout the dayside sector by several spacecraft located at distances corresponding to geosynchronous orbit and beyond. The timing of the perturbations observed by different spacecraft was found to be consistent with the motion of the FCB across the bow shock, in a dusk to dawn sense. Figure 1G) summarizes the reported downstream effects of FCBs.

## 5 Travelling foreshocks

TFs or foreshock cavities (e.g., Sibeck et al., 2002; Kajdič et al., 2017, See also Figure 1D) appear upstream of the bow shock, either in pristine SW or in the region of the ion foreshock that is not perturbed by the ULF waves. This happens when a bundle of magnetic field lines from a relatively thin magnetic flux tube, with orientation different from the background IMF, connects to the nominally quasi-perpendicular bow shock in such a way that the geometry of the section of the bow shock intersected by the flux tube is changed from quasi-perpendicular to quasi-parallel. As the flux tube is convected by the SW, its intersection with the bow shock propagates along the bow shock surface. Upstream of it, a foreshock is formed that follows this intersection. There are several ways that TFs may cause disturbances in the magnetosphere and the atmosphere (see also Figure 1G).

For example, it has been reported by Suvorova et al. (2019) that 2 TFs drove magnetospheric ULF waves in the Pc1 frequency band. Specifically, TFs caused ground Pc1 pearl pulsations, which are amplitude-modulated Pc1 waves with a repetition period of several tens of seconds (e.g., Jun et al., 2014). These pearl pulsations were observed for a long interval (~1 h) in the morning sector (4–8 local time, LT) and were detected at eight ground stations located at L = 3.5–7.4 (L is the distance expressed in $R_E$ at which the B-field lines cross the Earth's magnetic equator).

The same authors reported GOES-12 and THEMIS E measurements showing the Pc1 pulsations detected by the ground stations accompanied by EMIC waves in the frequency range 0.2–0.35 Hz in the prenoon sector (7.5–12 LT) at geocentric distances between 5.8 $R_E$ and 9 $R_E$. The events also caused precipitation of ions with energies 30–80 keV. Additionally, GOES-10 and 12 and THEMIS-B, -E and -D observed a transient compression of the dayside magnetosphere during which the magnetic field strength changed by up to 10 nT and whose observed durations were of up to 5 min.

Finally, Sibeck et al. (2021) and Kajdič et al. (2021) showed that TFs are directly transmitted into the magnetosheath where they can cause the formation of enhanced $P_{dyn}$ structures, known as magnetosheath jets (Plaschke et al., 2018), in the quasi-perpendicular magnetosheath. This is the region of the magnetosheath in which the jets are rarely observed and their origins are different from those detected in the quasi-paralell magnetosheath.

TABLE 1 Transient upstream mesoscale structures and observed downstream effects.

| | HFA | FB | FCB | TF |
|---|---|---|---|---|
| Magnetopause displacement | × | × | × | |
| Transient geomagnetic disturbances | × | × | × | |
| Transient magnetospheric plasma compression | | | × | |
| Transient deceleration of magnetospheric plasma | | | × | |
| Pc1 pulsations | | | | × |
| Pc3 pulsations | × | | | |
| Pc5 pulsations | × | × | | |
| Magnetospheric EMIC waves | | | | × |
| Ion precipitation | | | | × |
| Field-aligned currents | × | | | |
| Travelling convection vortices | × | | | |
| Ground magnetic field perturbations | × | × | | × |
| Auroral brightenings | × | | | |
| Magnetosheath jets | | | | × |

## 6 Summary and discussion

In this mini-review we discussed the reported downstream effects of the four largest-scale TUMS on the near-Earth environment. These structures may strongly affect the bow shock–magnetosheath–ionosphere system and create a wide range of space weather phenomena. It is almost certain that in the future the list of impacts of each type of TUMS will keep increasing. Table 1 summarizes explicitly reported space weather effects.

We still do not understand all the mechanisms by which different TUMS affect the regions downstream of the bow shock.

For example, we do not know how the monochromatic Pc3 fluctuations are caused by HFAs. One possibility is that shocks that sometimes form at the HFAs and FBs steepened edges, drive their own foreshocks with ULF fluctuations which eventually perturb the magnetosphere, similar to the ULF waves in the terrestrial foreshock (e.g., Engebretson et al., 1987; Turc et al., 2023). Turbulence and waves in the cores of these structures (Zhang et al., 2010b; Kovács et al., 2014) could also be the cause.

Another possible effect that has not yet been well studied is that TUMS associated enhancements of $P_{dyn}$ could lead to impulsive penetration of mass into the magnetosphere (Dmitriev and Suvorova, 2015). Modification of the IMF upstream and in the magnetosheath could also result in magnetopause reconnection (Hietala et al., 2018).

These effects could be caused by TUMS associated magnetosheath jets (Plaschke et al., 2018). It has been shown by Sibeck et al. (2021) and Kajdič et al. (2021) that the TFs transmitted into the magnetosheath can be a source of these jets downstream of the quasi-perpendicular bow-shock. Nykyri et al. (2019), Dmitriev and Suvorova (2023) have demonstrated that magnetosheath jets can be geoeffective and can act as a vector for coupling TUMS and foreshock processes to the magnetopause and ionosphere.

To make matter worse, certain types of TUMS can contain another type of upstream mesoscale structures. The latter is most evident in the case of TFs that often contain FCBs at their edges (Kajdič et al., 2017). Moreover, TFs exhibit other phenomena that are also observed inside the "regular" foreshock, such as ULF waves, shocklets, foreshock cavitons, etc.

## 7 Future work

It is clear that our knowledge of how exactly TUMS interact with the bow shock and the regions downstream of it is still limited. Future investigations should include more multi-point observations of individual events with spacecraft in different regions (upstream of the bow shock, magnetosheath, magnetosphere, ground observations). These should be accompanied by local and global numerical simulations. There are numerous tasks in the "to do" list:

- Study of the microphysics in the cores and the boundary regions of the TUMS, i.e., possible generation of ULF waves and turbulence, magnetic reconnection, particle heating and acceleration.
- Study of the impact of foreshock cavitons and spontaneous hot flow anomalies on the regions downstream of the terrestrial bow-shock.
- Comparison study of properties and impact if FBs formed by rotational *versus* tangential discontinuities.
- Detailed investigations of the impact of the TUMS on the bow shock. Do TUMS cause shock erosion, its additional rippling and what are the downstream consequences of these processes?
- Studies of the TUMS's substructure and the physical processes leading to it.
- Direct observational confirmation between the TFs and the magnetosheath jets and Pc3–4 waves in the magnetosphere.
- Statistical study that would reveal the relative importance of travelling *versus* the "regular" foreshocks for the production of magnetosheath jets and Pc3–4 waves.
- Determine the impact of each type of TUMS on the nightside magnetosphere. For example, can they trigger substorms?
- Test whether energetic particles accelerated in the foreshock and TUMS can enter into the magnetosphere (across the magnetopause or through the cusp) and become geoeffective.

- Quantify the energy input from TUMS into the magnetosphere in comparison with typical solar wind drivers.
- Determine the role of TUMS during storm time (e.g., enhance magnetospheric ULF waves and thus modulate radiation belt particles).
- Determine how HFAs excite the Pc3 waves and whether they can also be caused by FBs.
- Determine the impact of TUMS on the near-planetary environment at other planets. One such opportunity will emerge with the dual orbiter BepiColombo mission at Mercury.

Such tasks require multi-point spacecraft observations as well as 3D physically scaled global numeric models that go beyond the fluid description of plasma. Currently, numerous *in situ* and ground based observations are available as well as the required kinetic simulation assets that will make addressing these tasks possible.

## Author contributions

PK: Visualization, Writing–original draft, Writing–review and editing. XB-C: Writing–original draft, Writing–review and editing. LT: Writing–original draft, Writing–review and editing. MA: Writing–original draft, Writing–review and editing. SR: Writing–original draft, Writing–review and editing. TL: Writing–original draft, Writing–review and editing. YP-K: Writing–original draft, Writing–review and editing. AL: Writing–original draft, Writing–review and editing. YH: Writing–original draft, Writing–review and editing. PE: Writing–original draft, Writing–review and editing. NO: Writing–original draft, Writing–review and editing. DS: Writing–original draft, Writing–review and editing. BW: Writing–original draft, Writing–review and editing. HZ: Writing–original draft, Writing–review and editing. YL: Writing–original draft, Writing–review and editing.

## Funding

The author(s) declare financial support was received for the research, authorship, and/or publication of this article. This work was supported by the International Space Science Institute (ISSI) through ISSI International Team project #555. PK's work was supported by the DGAPA PAPIIT through the IN100424 grant. XB-C acknowledges DGAPA PAPIIT grant IN106724. The work of LT was supported by the Research Council of Finland (grant number 322544). SR acknowledges funding from NASA DRIVE Science Center for Geospace Storms (CGS) — 80NSSC22M0163. DS's work was supported by NASA's LWS TR&T program. MOA was supported by UKRI (STFC/EPSRC) Stephen Hawking Fellowship EP/T01735X/1 and UKRI Future Leaders Fellowship MR/X034704/1. YP-K acknowledges Academy of Finland grant no. 339756. AL was supported by Royal Society awards URF\R1\180671 and RGF\EA\181090. HZ acknowledges National Natural Science Foundation of China grant 42330202.

## Acknowledgments

The ClWeb (https://clweb.irap.omp.eu/) tool was used for visualizing the data and producing some of the figures.

## Conflict of interest

Author NO was employed by Solana Scientific Inc.

The remaining authors declare that the research was conducted in the absence of any commercial or financial relationships that could be construed as a potential conflict of interest.

The author(s) declared that they were an editorial board member of Frontiers, at the time of submission. This had no impact on the peer review process and the final decision.

## Publisher's note



## References

Akasofu, S.-I. (2021). A review of studies of geomagnetic storms and auroral/magnetospheric substorms based on the electric current approach. *Front. Astronomy Space Sci.* 7, 100. doi:10.3389/fspas.2020.604750

Anderson, B. J., and Hamilton, D. C. (1993). Electromagnetic ion cyclotron waves stimulated by modest magnetospheric compressions. *J. Geophys. Res.* 98, 11369–11382. doi:10.1029/93JA00605

Araki, T. (1994). *A physical model of the geomagnetic sudden commencement*. Washington, D. C: AGU, 183–200. doi:10.1029/GM081p0183

Archer, M. O., Turner, D. L., Eastwood, J. P., Horbury, T. S., and Schwartz, S. J. (2014). The role of pressure gradients in driving sunward magnetosheath flows and magnetopause motion. *J. Geophys. Res.* 119, 8117–8125. doi:10.1002/2014JA020342

Archer, M. O., Turner, D. L., Eastwood, J. P., Schwartz, S. J., and Horbury, T. S. (2015). Global impacts of a Foreshock Bubble: magnetosheath, magnetopause and ground-based observations. *Planet. Space Sci.* 106, 56–66. doi:10.1016/j.pss.2014.11.026

Borodkova, N. L., Sibeck, D. G., Zastenker, G. N., Romanov, S. A., and Sauvaud, J. A. (1998). Fast deformation of dayside magnetopause. *Cosmic Res.* 36, 245.

Borovsky, J. E. (2008). Flux tube texture of the solar wind: strands of the magnetic carpet at 1 AU? *J. Geophys. Res.* 113, A08110. doi:10.1029/2007JA012684

Chu, C., Zhang, H., Sibeck, D., Otto, A., Zong, Q., Omidi, N., et al. (2017). THEMIS satellite observations of hot flow anomalies at Earth's bow shock. *Ann. Geophys.* 35, 443–451. doi:10.5194/angeo-35-443-2017

Collinson, G., Halekas, J., Grebowsky, J., Connerney, J., Mitchell, D., Espley, J., et al. (2015). A hot flow anomaly at mars. *Geophys. Res. Lett.* 42, 9121–9127. doi:10.1002/2015GL065079

Collinson, G., Sibeck, D., Omidi, N., Frahm, R., Zhang, T., Mitchell, D., et al. (2020). Foreshock cavities at venus and mars. *J. Geophys. Res. Space Phys.* 125, e2020JA028023. doi:10.1029/2020JA028023

Collinson, G. A., Sibeck, D. G., Masters, A., Shane, N., Zhang, T. L., Fedorov, A., et al. (2014). A survey of hot flow anomalies at venus. *J. Geophys. Res. Space Phys.* 119, 978–991. doi:10.1002/2013JA018863

Collinson, G. A., Wilson, L. B., III, Sibeck, D. G., Shane, N., Zhang, T. L., Moore, T. E., et al. (2012). Short large-amplitude magnetic structures (SLAMS) at Venus. *J. Geophys. Res.* 117, A10221. doi:10.1029/2012JA017838

Dmitriev, A. V., and Suvorova, A. V. (2015). Large-scale jets in the magnetosheath and plasma penetration across the magnetopause: THEMIS observations. *J. Geophys. Res.* 120, 4423–4437. doi:10.1002/2014JA020953

Dmitriev, A. V., and Suvorova, A. V. (2023). Atmospheric effects of magnetosheath jets. *Atmosphere* 14, 45. doi:10.3390/atmos14010045

Eastwood, J. P., Balogh, A., Lucek, E. A., Mazelle, C., and Dandouras, I. (2005). Quasi-monochromatic ulf foreshock waves as observed by the four-spacecraft cluster mission: 1. statistical properties. *J. Geophys. Res. Space Phys.* 110. doi:10.1029/2004JA010617

Eastwood, J. P., Biffis, E., Hapgood, M. A., Green, L., Bisi, M. M., Bentley, R. D., et al. (2017). The economic impact of space weather: where do we stand? *Risk Anal.* 37, 206–218. doi:10.1111/risa.12765

Eastwood, J. P., Schwartz, S. J., Horbury, T. S., Carr, C. M., Glassmeier, K.-H., Richter, I., et al. (2011). Transient pc3 wave activity generated by a hot flow anomaly: cluster, rosetta, and ground-based observations. *J. Geophys. Res. Space Phys.* 116. doi:10.1029/2011JA016467

Engebretson, M. J., Zanetti, L. J., Potemra, T. A., Baumjohann, W., Luehr, H., and Acuna, M. H. (1987). Simultaneous observation of Pc 3-4 pulsations in the solar wind and in the Earth's magnetosphere. *J. Geophys. Res.* 92, 10053–10062. doi:10.1029/JA092iA09p10053

Facskó, G., Opitz, A., Lavraud, B., Luhmann, J., Russell, C., Sauvaud, J.-A., et al. (2015). Hot flow anomaly remnant in the far geotail? *J. Atmos. Solar-Terrestrial Phys.* 124, 39–43. doi:10.1016/j.jastp.2015.01.011

Glassmeier, K. H., Motschmann, U., Dunlop, M., Balogh, A., Acuña, M. H., Carr, C., et al. (2001). Cluster as a wave telescope - first results from the fluxgate magnetometer. *Ann. Geophys.* 19, 1439–1447. doi:10.5194/angeo-19-1439-2001

Greenstadt, E. W., Le, G., and Strangeway, R. J. (1995). ULF waves in the foreshock. *Adv. Space Res.* 15, 71–84. doi:10.1016/0273-1177(94)00087-H

Hartinger, M. D., Turner, D. L., Plaschke, F., Angelopoulos, V., and Singer, H. (2013). The role of transient ion foreshock phenomena in driving Pc5 ULF wave activity. *J. Geophys. Res. (Space Phys.)* 118, 299–312. doi:10.1029/2012JA018349

Hietala, H., Phan, T. D., Angelopoulos, V., Oieroset, M., Archer, M. O., Karlsson, T., et al. (2018). *In situ* observations of a magnetosheath high-speed jet triggering magnetopause reconnection. *Geophys. Res. Lett.* 45, 1732–1740. doi:10.1002/2017GL076525

Jacobs, J. A., Kato, Y., Matsushita, S., and Troitskaya, V. A. (1964). Classification of geomagnetic micropulsations. *J. Geophys. Res.* 69, 180–181. doi:10.1029/JZ069i001p00180

Jacobsen, K. S., Phan, T. D., Eastwood, J. P., Sibeck, D. G., Moen, J. I., Angelopoulos, V., et al. (2009). THEMIS observations of extreme magnetopause motion caused by a hot flow anomaly. *J. Geophys. Res.* 114, A08210. doi:10.1029/2008JA013873

Jun, C.-W., Shiokawa, K., Connors, M., Schofield, I., Poddelsky, I., and Shevtsov, B. (2014). Study of Pc1 pearl structures observed at multi-point ground stations in Russia, Japan, and Canada. *Earth, Planets Space* 66, 140. doi:10.1186/s40623-014-0140-8

Kajdič, P., Blanco-Cano, X., Omidi, N., Rojas-Castillo, D., Sibeck, D. G., and Billingham, L. (2017). Traveling foreshocks and transient foreshock phenomena. *J. Geophys. Res. Space Phys.* 122, 9148–9168. doi:10.1002/2017JA023901

Kajdič, P., Raptis, S., Blanco-Cano, X., and Karlsson, T. (2021). Causes of jets in the quasi-perpendicular magnetosheath. *Geophys. Res. Lett.* 48, e2021GL093173. doi:10.1029/2021GL093173

Kilpua, E. K. J., Balogh, A., von Steiger, R., and Liu, Y. D. (2017). Geoeffective properties of solar transients and stream interaction regions. *Space Sci. Rev.* 212, 1271–1314. doi:10.1007/s11214-017-0411-3

Kovács, P., Facskó, G., and Dandouras, I. (2014). Turbulent dynamics inside the cavity of hot flow anomaly. *Planet. Space Sci.* 92, 24–33. doi:10.1016/j.pss.2014.01.001

Li, W., Thorne, R. M., Bortnik, J., Nishimura, Y., and Angelopoulos, V. (2011). Modulation of whistler mode chorus waves: 1. role of compressional pc4–5 pulsations. *J. Geophys. Res. Space Phys.* 116. doi:10.1029/2010JA016312

Liu, T. Z., Turner, D. L., Angelopoulos, V., and Omidi, N. (2016). Multipoint observations of the structure and evolution of foreshock bubbles and their relation to hot flow anomalies. *J. Geophys. Res.* 121, 5489–5509. doi:10.1002/2016JA022461

Liu, T. Z., Wang, C.-P., Wang, B., Wang, X., Zhang, H., Lin, Y., et al. (2020). ARTEMIS observations of foreshock transients in the midtail foreshock. *Geophys. Res. Lett.* 47, e90393. doi:10.1029/2020GL090393

Liu, T. Z., Zhang, H., Wang, C.-P., Angelopoulos, V., Vu, A., Wang, X., et al. (2021). Statistical study of foreshock transients in the midtail foreshock. *J. Geophys. Res. (Space Phys.)* 126, e29156. doi:10.1029/2021JA029156

Liu, Z., Turner, D. L., Angelopoulos, V., and Omidi, N. (2015). THEMIS observations of tangential discontinuity-driven foreshock bubbles. *Geophys. Res. Lett.* 42, 7860–7866. doi:10.1002/2015GL065842

Madanian, H., Omidi, N., Sibeck, D. G., Andersson, L., Ramstad, R., Xu, S., et al. (2023). Transient foreshock structures upstream of mars: implications of the small martian bow shock. *Geophys. Res. Lett.* 50, e2022GL101734. doi:10.1029/2022GL101734

Masters, A., Arridge, C. S., Dougherty, M. K., Bertucci, C., Billingham, L., Schwartz, S. J., et al. (2008). Cassini encounters with hot flow anomaly-like phenomena at saturn's bow shock. *Geophys. Res. Lett.* 35. doi:10.1029/2007GL032371

Nishimura, Y., Kikuchi, T., Ebihara, Y., Yoshikawa, A., Imajo, S., Li, W., et al. (2016). Evolution of the current system during solar wind pressure pulses based on aurora and magnetometer observations. *Earth, Planets Space* 68, 144. doi:10.1186/s40623-016-0517-y

Nykyri, K., Bengtson, M., Angelopoulos, V., Nishimura, Y., and Wing, S. (2019). Can enhanced flux loading by high-speed jets lead to a substorm? Multipoint detection of the christmas day substorm onset at 08:17 UT, 2015. *J. Geophys. Res. (Space Phys.)* 124, 4314–4340. doi:10.1029/2018JA026357

Øieroset, M., Mitchell, D. L., Phan, T. D., Lin, R. P., and Acuña, M. H. (2001). Hot diamagnetic cavities upstream of the Martian bow shock. *Geophys. Res. Lett.* 28, 887–890. doi:10.1029/2000GL012289

Olson, J. V., and Lee, L. C. (1983). Pc1 wave generation by sudden impulses. *Planet. Space Sci.* 31, 295–302. doi:10.1016/0032-0633(83)90079-X

Omidi, N., Collinson, G., and Sibeck, D. (2020). Foreshock bubbles at venus: hybrid simulations and vex observations. *J. Geophys. Res. Space Phys.* 125, e2019JA027056. doi:10.1029/2019JA027056

Omidi, N., Eastwood, J. P., and Sibeck, D. G. (2010). Foreshock bubbles and their global magnetospheric impacts. *J. Geophys. Res.* 115, A06204. doi:10.1029/2009JA014828

Omidi, N., Sibeck, D. G., and Blanco-Cano, X. (2009). Foreshock compressional boundary. *J. Geophys. Res.* 114, A08205. doi:10.1029/2008JA013950

Paschmann, G., Sckopke, N., Asbridge, J., Bame, S., and Gosling, J. (1980). Energization of solar wind ions by reflection from the earth's bow shock. *J. Geophys. Res. Space Phys.* 85, 4689–4693. doi:10.1029/JA085iA09p04689

Plaschke, F., Hietala, H., Archer, M., Blanco-Cano, X., Kajdič, P., Karlsson, T., et al. (2018). Jets downstream of collisionless shocks. *Space Sci. Rev.* 214, 81. doi:10.1007/s11214-018-0516-3

Šafránková, J., Goncharov, O., Němeček, Z., Přech, L., and Sibeck, D. G. (2012). Asymmetric magnetosphere deformation driven by hot flow anomaly(ies). *Geophys. Res. Lett.* 39, L15107. doi:10.1029/2012GL052636

Schwartz, S. J., Chaloner, C. P., Christiansen, P. J., Coates, A. J., Hall, D. S., Johnstone, A. D., et al. (1985). An active current sheet in the solar wind. *Nature* 318, 269–271. doi:10.1038/318269a0

Shen, X.-C., Shi, Q., Wang, B., Zhang, H., Hudson, M. K., Nishimura, Y., et al. (2018). Dayside magnetospheric and ionospheric responses to a foreshock transient on 25 june 2008: 1. flr observed by satellite and ground-based magnetometers. *J. Geophys. Res. Space Phys.* 123, 6335–6346. doi:10.1029/2018JA025349

Shi, R., Hu, Z.-J., Ni, B., Han, D., Chen, X.-C., Zhou, C., et al. (2014). Modulation of the dayside diffuse auroral intensity by the solar wind dynamic pressure. *J. Geophys. Res. (Space Phys.)* 119, 10092–10099. doi:10.1002/2014JA020180

Shuvalov, S., Ermakov, V., Zorina, V., and Kim, K. (2019). Propagation properties of hot flow anomalies at mars: maven observations. *Planet. Space Sci.* 179, 104717. doi:10.1016/j.pss.2019.104717

Sibeck, D. G., Borodkova, N. L., Schwartz, S. J., Owen, C. J., Kessel, R., Kokubun, S., et al. (1999). Comprehensive study of the magnetospheric response to a hot flow anomaly. *J. Geophys. Res.* 104, 4577–4594. doi:10.1029/1998JA900021

Sibeck, D. G., Borodkova, N. L., Zastenker, G. N., Romanov, S. A., and Sauvaud, J.-A. (1998). Gross deformation of the dayside magnetopause. *Geophys. Res. Lett.* 25, 453–456. doi:10.1029/98GL00134

Sibeck, D. G., Lee, S. H., Omidi, N., and Angelopoulos, V. (2021). Foreshock cavities: direct transmission through the bow shock. *J. Geophys. Res. (Space Phys.)* 126, e29201. doi:10.1029/2021JA029201

Sibeck, D. G., Phan, T.-D., Lin, R., Lepping, R. P., and Szabo, A. (2002). Wind observations of foreshock cavities: a case study. *J. Geophys. Res.* 107, 1271. doi:10.1029/2001JA007539

Sitar, R. J., Baker, J. B., Clauer, C. R., Ridley, A. J., Cumnock, J. A., Papitashvili, V. O., et al. (1998). Multi-instrument analysis of the ionospheric signatures of a hot flow anomaly occurring on july 24, 1996. *J. Geophys. Res. Space Phys.* 103, 23357–23372. doi:10.1029/98JA01916

Slavin, J. A., Acuña, M. H., Anderson, B. J., Barabash, S., Benna, M., Boardsen, S. A., et al. (2009). MESSENGER and Venus Express observations of the solar wind interaction with Venus. *Geophys. Res. Lett.* 36, L09106. doi:10.1029/2009GL037876

Suvorova, A. V., Dmitriev, A. V., Parkhomov, V. A., and Tsegmed, B. (2019). Quiet time structured Pc1 waves generated during transient foreshock. *J. Geophys. Res. (Space Phys.)* 124, 9075–9093. doi:10.1029/2019JA026936

Takahashi, K., McPherron, R. L., and Terasawa, T. (1984). Dependence of the spectrum of Pc 3-4 pulsations on the interplanetary magnetic field. *J. Geophys. Res. Space Phys.* 89, 2770–2780. doi:10.1029/JA089iA05p02770

Thomsen, M. F., Gosling, J. T., Fuselier, S. A., Bame, S. J., and Russell, C. T. (1986). Hot, diamagnetic cavities upstream from the earth's bow shock. *J. Geophys. Res. Space Phys.* 91, 2961–2973. doi:10.1029/JA091iA03p02961

Tsyganenko, N. A. (2014). Data-based modeling of the geomagnetosphere with an IMF-dependent magnetopause. *J. Geophys. Res. (Space Phys.)* 119, 335–354. doi:10.1002/2013JA019346

Turc, L., Roberts, O. W., Verscharen, D., Dimmock, A. P., Kajdič, P., Palmroth, M., et al. (2023). Transmission of foreshock waves through Earth's bow shock. *Nat. Phys.* 19, 78–86. doi:10.1038/s41567-022-01837-z

Turner, D. L., Liu, T. Z., Wilson, L. B., Cohen, I. J., Gershman, D. G., Fennell, J. F., et al. (2020). Microscopic, multipoint characterization of foreshock bubbles with magnetospheric multiscale (MMS). *J. Geophys. Res. (Space Phys.)* 125, e27707. doi:10.1029/2019JA027707

Uritsky, V. M., Slavin, J. A., Boardsen, S. A., Sundberg, T., Raines, J. M., Gershman, D. J., et al. (2014). Active current sheets and candidate hot flow anomalies upstream of mercury's bow shock. *J. Geophys. Res. Space Phys.* 119, 853–876. doi:10.1002/2013ja0190522013JA019052

Valek, P. W., Thomsen, M. F., Allegrini, F., Bagenal, F., Bolton, S., Connerney, J., et al. (2017). Hot flow anomaly observed at jupiter's bow shock. *Geophys. Res. Lett.* 44, 8107–8112. doi:10.1002/2017GL073175

Wang, C.-P., Liu, T. Z., Xing, X., and Masson, A. (2018). Multispacecraft observations of tailward propagation of transient foreshock perturbations to midtail magnetosheath. *J. Geophys. Res. Space Phys.* 123, 9381–9394. doi:10.1029/2018JA025921

Wang, C.-P., Wang, X., Liu, T. Z., and Lin, Y. (2020). Evolution of a foreshock bubble in the midtail foreshock and impact on the magnetopause: 3-d global hybrid simulation. *Geophys. Res. Lett.* 47, e2020GL089844. doi:10.1029/2020GL089844

Wang, C.-P., Wang, X., Liu, T. Z., and Lin, Y. (2021). A foreshock bubble driven by an imf tangential discontinuity: 3d global hybrid simulation. *Geophys. Res. Lett.* 48, e2021GL093068. doi:10.1029/2021GL093068

Zhang, H., Sibeck, D. G., Zong, Q. G., Gary, S. P., McFadden, J. P., Larson, D., et al. (2010a). Time History of Events and Macroscale Interactions during Substorms observations of a series of hot flow anomaly events. *J. Geophys. Res. (Space Phys.)* 115, A12235. doi:10.1029/2009JA015180

Zhang, H., and Zong, Q. (2020). *Transient phenomena at the magnetopause and bow shock and their ground signatures.* AGU, 11–37. doi:10.1002/9781119509592.ch2

Zhang, X. Y., Zong, Q.-G., Wang, Y. F., Zhang, H., Xie, L., Fu, S. Y., et al. (2010b). Ulf waves excited by negative/positive solar wind dynamic pressure impulses at geosynchronous orbit. *J. Geophys. Res. Space Phys.* 115. doi:10.1029/2009ja0150162009JA015016

Zhao, L. L., Zhang, H., and Zong, Q. G. (2017). Global ULF waves generated by a hot flow anomaly. *Geophys. Res. Lett.* 44, 5283–5291. doi:10.1002/2017GL073249

Zong, Q. (2010). Energetic electrons response to ULF waves induced by interplanetary shocks in the outer radiation belt. in *38th COSPAR scientific assembly. Vol. 38, 2.*